Design, Synthesis, Physicochemical and Drug-Likeness Properties of Quercetin Derivatives and their Effect on MCF-7 Cell Line and Free Radicals

Sulakshana Shankar[1], Jaishree Vaijanathappa[2*], Ashish Wadhwani[3], Mahendran Sekar[4]

[1]Department of Pharmaceutical Chemistry, JSS College of Pharmacy, JSS Academy of Higher Education and Research, Mysuru-570015, Karnataka, India; [2]Department of Life Sciences, JSS Academy of Higher Education and Research, Vacoas-Phoenix, Mauritius; [3]Department of Health Sciences, JSS Academy of Higher Education and Research, Vacoas-Phoenix, Mauritius; [4]Department of Pharmaceutical Chemistry, Universiti Kuala Lumpur Royal College of Medicine Perak, Ipoh-30450, Perak, Malaysia

ABSTRACT

In the present study, four novel quercetin derivatives were designed and synthesized by one pot synthesis method using benzoic acid and its derivatives. The synthesized compounds were screened for physicochemical and drug-likeness properties, evaluated for *in vitro* antioxidant assays such as Hydrogen Peroxide (H_2O_2) and 2,2-Diphenyl-1-Picryl Hydrazyl (DPPH), cytotoxicity study on breast cancer cell line MCF-7 and performed molecular docking against the inducible Nitric Oxide Synthase (iNOS) enzyme 4 NOS PDB (Protein Data Bank) ID which is expressed in breast cancer. In the screening of physicochemical and drug-likeness properties, QB, QB1 and QB4 are eligible for oral drug screening and other derivatives QB2 and QB3 were not eligible for oral drug screening. Among all, QB-1 showed the highest percentage of inhibition and the lowest IC_{50} value in both assays. The docking results displayed that QB-2 showed the highest docking score and exhibited the highest cytotoxicity against the MCF-7 cell line and the study results conclude that QB1 and QB2 compounds can be further explored for *in vivo* anticancer activity.

Keywords: Quercetin derivatives; Drug-likeness; Physicochemical properties; Antioxidant activity; Cytotoxicity; Molecular docking

INTRODUCTION

The generation of free radicals is a key factor that can lead to the development of various diseases related to the central nervous system, cardiovascular system, respiratory, skeletal, excretory systems, metabolism and multi-organs. These free radicals are either produced endogenously due to inflammation, stress, immune cell activation, ischemia, exercise, infection, aging, cancer or through exogenous substances such as cigarette smoking, alcohol consumption, heavy and transition metals, pharmaceutical agents, radiation and air and water pollutants [1]. Flavonols, the largest subclass of flavonoids is widely found in fruits and vegetables such as grapes, berries, apples, broccoli, onions and citrus fruits. They are characterized by the presence of a ketone group at C_4 along with an unsaturation between the C_2 and C_3 position and a hydroxyl group at C_3 in the C ring. Quercetin is one of the most common flavonol present in several plant foods. Structurally, quercetin is 3,5,7,3',4'-pentahydroxyflavone (2-(3,4-dihydroxyphenyl)-3,5,7-trihydroxy-4H-chromen-4-one) and the presence of five hydroxyl groups is responsible for its versatile biological activities such as antioxidant, anticancer, antimicrobial, anti-inflammatory and

for treating age-related, cardiovascular and neurodegenerative disorders (Figure 1) [2,3].
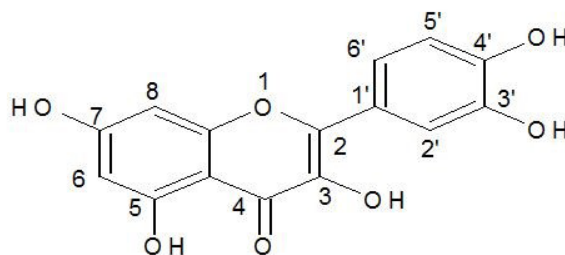
Figure 1: Structure of quercetin.

Quercetin can exhibit radical scavenging activity for the protection of body cells against free radicals that are produced during the metabolism process or from external sources such as pollution, cigarette smoke, radiation and medication. Perhaps, according to the studies, quercetin faces limitations regarding its bioavailability due to poor absorption of quercetin because of low solubility of

Citation: Shankar S, Vaijanathappa J, Wadhwani A, Sekar M (2023) Design, Synthesis, Physicochemical and Drug-Likeness Properties of Quercetin Derivatives and their Effect on MCF-7 Cell Line and Free Radicals. J Clin Toxicol. 13:547.

quercetin and the first-pass effect of quercetin in the liver and gut [4,5]. Studies have shown that the introduction of the ester group into the quercetin scaffold has produced potent compounds for antioxidant, and anticancer (anti-proliferative) and enhanced the bioavailability as well [6]. Danihelová, et al. [7], prepared fifteen quercetin-derived compounds by condensation or selective protection reactions followed by acyl chloride acylation, which showed strong cytotoxicity towards HeLa cells [7]. Other quercetin derivatives synthesized by esterification with aspirin at the 3- and 7-OH groups reported for higher cytotoxic effects against liver (HepG2) and promyelocytic leukemia (HL-60) cancer cells [8], and anti-hepatitis C virus activity [9]. Hence, chemical modification of quercetin can generate novel derivatives with improved biological effects, bioavailability and solubility properties. Therefore, in the present study we aimed for one-pot synthesis of quercetin esters, physicochemical and drug-likeness properties, molecular docking and its biological evaluation.

MATERIALS AND METHODS

Experimental

Chemistry: All the chemicals, reagents and solvents used for experimental work were analytical grade. The formation of the product was monitored by performing TLC (using silica gel F254 aluminium sheets from Merck Company). Column chromatography was carried out by using silica gel 100-200 mesh. An open capillary method was performed to determine the melting point of the synthesised quercetin derivatives and was expressed in units of °C. IR spectral study was carried out using Shimadzu FTIR 8400-S spectrophotometer by KBr Press method and IR data obtained was expressed in cm^{-1}. ^{1}H NMR and ^{13}C NMR studies were carried out on Bruker 400 MHz FT-NMR spectrophotometer using trimethylsilane as internal standard and DMSO (D$_6$) and CDCl$_3$ as solvent systems. Mass spectra were recorded on LC-MS ACQUITY UPLC mass spectrometer using AP and ESI method and TOF detector.

Synthesis of quercetin derivatives

Synthesis of 2-(3,4-dihydroxyphenyl)-5,7-dihydroxy-4-oxo-4H-chromen-3-yl benzoate (QB1): Quercetin dihydrate (2 mmol), benzoic acid (6 mmol) and zinc chloride (2 mmol) were taken in a RBF. 10 ml of phosphorous oxychloride was gradually added to the mixture and was stirred for 15 hrs at 75°C. The reaction completion was supervised by Thin Layer Chromatography (TLC). Upon formation of the product, stopped stirring and the product was allowed to cool. Ice cold water was added and then product was extracted using ethyl acetate [10]. The separated ethyl acetate layer was collected and evaporated. The obtained brownish yellow product was subjected to preparative TLC, using chloroform: methanol (70:30) as the mobile phase. The pure product was separated, collected and dried. Yield: 80 mg (10%); m.p. 220-223°C; FT-IR (cm^{-1}): 3360.11 (alcohol O-H stretch), 3070.78 (Ar-H), 1695.49 (C=O stretch), 1506.46 (C=C stretch), 1174.59 (C-O ester); ^{1}H NMR (400 MHz (D6)DMSO): δ 6.18 (s, ^{1}H, ArH($_6$)), 6.45 (s, ^{1}H, ArH($_8$)), 7.13 (d, J=6.4 Hz, ^{1}H, ArH($_{14}$)), 7.47 (s, ^{1}H, ArH($_{11}$)), 7.59 (t, J=2.4 Hz, ^{2}H, ArH($_{19}$)), 7.74 (d, J=5.6 Hz, ^{1}H, ArH($_{15}$)), 7.93 (t, J=8.4 Hz, ^{1}H, ArH($_{20}$)), 8.13 (d, J=3.2 Hz, ^{2}H ArH($_{18}$)), 9.32 (s, ^{3}H, OH($_{7,12,13}$)), 12.46 (s, ^{1}H, OH(5)); ^{13}C NMR (400 MHz (D6) DMSO): δ 93.97 (C$_8$), 98.85 (C$_6$), 104.89 (C$_4$), 113.24 (C$_{11}$), 116.15 (C$_{14}$), 122.72 (C$_{15}$), 124.32 (C$_{10}$), 128.97 (C$_{19}$), 129.39 (C$_{18}$), 129.7

(C$_2$), 130.1 (C$_{20}$), 130.33 (C$_{17}$), 131.4 (C$_{12}$), 133.2 (C$_{13}$), 155.81 (C$_1$), 157.95 (C$_9$), 161.12 (C$_7$), 164.21 (C$_{16}$), 164.53 (C$_7$), 167.86 (C$_3$); LC-MS, m/z: calculated for C$_{22}$H$_{14}$O$_8$ is 406.07; found 407.01 (M+H)$^+$.

Synthesis of 2-(3,4-dihydroxyphenyl)-7-hydroxy-4-oxo-4H-chromene-3,5-diyl bis(2-chlorobenzoate) (QB2): Quercetin dihydrate (2 mmol), 2-chlorobenzoic acid (5 mmol) and zinc chloride (2 mmol) were taken in a Round Bottom Flask (RBF). Then, 10 ml of phosphorous oxychloride was gradually added to the reaction mixture and stirred for 15 hrs at 75°C. The reaction completion was supervised by Thin Layer Chromatography (TLC). Upon formation of the product, stopped stirring and the product was allowed to cool. Ice cold water was added to the mixture and product was extracted using ethyl acetate. The separated ethyl acetate layer was collected and evaporated [10]. The obtained yellow product was subjected to preparative TLC, using chloroform: methanol (60:40) as the mobile phase. The pure product was separated, collected and dried. Yield: 100 mg (8.7%); m.p. 230-232°C; FT-IR (cm^{-1}): 3344.68 (alcohol O-H stretch), 2924.18 (Ar–H), 1726.35 (C=O stretch), 1654.99 (C=C stretch), 1172.76 (C-O ester), 725.78 (C-Cl); ^{1}H NMR (400 MHz (D$_6$)DMSO): δ 6.037 (s, ^{1}H, ArH($_8$)), 6.179 (s, ^{1}H, ArH($_6$)), 6.45 (s, ^{1}H, ArH($_{11}$)), 6.72 (d, J=4.4 Hz, ^{1}H, ArH($_{14}$)), 7.20 (d, J=3.6 Hz, ^{1}H, ArH($_{15}$)), 7.69 (t, J=8 Hz, ^{4}H, ArH($_{20,21}$)), 8.08 (d, J=10.4 Hz, ^{2}H ArH($_{19}$)), 8.23 (d, J=2.4 Hz, ^{2}H ArH($_{22}$)), 9.375 (s, ^{3}H, OH($_{7,12,13}$)); ^{13}C NMR (400 MHz (D6)DMSO): δ 94.43 (C$_8$), 98.95 (C$_6$), 102.12 (C$_4$), 114.97 (C$_{14}$), 115.08 (C$_{11}$), 119.87 (C$_{10}$), 121.27 (C$_{15}$), 128.02 (C$_{21}$), 129.41 (C$_{17}$), 129.76 (C$_{20}$), 130.87 (C$_{19}$), 131.65 (C$_{22}$), 133.59 (C$_{18}$), 141.73 (C$_2$), 144.58 (C$_{12}$), 144.67 (C$_{13}$), 147.58 (C$_5$), 153.33 (C$_1$), 153.42 (C$_9$), 160.16 (C$_7$), 166.21 (C$_{16}$), 174.03 (C$_3$); LC-MS, m/z:exact mass calculated for C$_{29}$H$_{16}$C$_{12}$O$_9$ is 578.02; found 578.85.

Synthesis of 2-(3,4-dihydroxyphenyl)-7-hydroxy-4-oxo-4H-chromene-3,5-diyl bis(4-chlorobenzoate) (QB3): The quercetin dihydrate (3 mmol), 4-chlorobenzoic acid (8 mmol) and zinc chloride (3 mmol) were transferred in an RBF. Then 10 ml of phosphorous oxychloride was gradually added and the reaction mixture was stirred for 15 hrs at 75°C. The reaction completion was monitored by TLC and upon formation of the product the reaction was stopped and the mixture was allowed to cool. Ice cold water was added and then extracted using ethyl acetate. The separated ethyl acetate layer was collected and evaporated. The obtained pale yellow product was subjected to column chromatography using dichloromethane: ethyl acetate (50:50) as the mobile phase. The pure product was separated, collected, and dried. Yield: 154 mg (9 %); m.p. 240-242 °C; FT-IR (cm^{-1}): 3363.97 (alcohol O-H stretch), 2924.18 (Ar-H), 1743.71 (C=O stretch), 1687.77 (C=C stretch), 1139.97 (C-O ester), 725.82 (C-Cl); ^{1}H NMR (400 MHz CDCl$_3$): δ 6.07 (s, ^{1}H, ArH($_8$)), 6.25 (s, ^{1}H, ArH($_6$)), 6.54 (s, ^{1}H, ArH($_{11}$)), 6.85 (d, J = 5.6 Hz, ^{1}H, ArH($_{14}$)), 7.25 (d, J=4.8 Hz, ^{1}H, ArH($_{15}$)), 7.51 (d, J=2.4 Hz, ^{2}H, ArH($_{24}$)), 7.74 (d, J=2 Hz, ^{2}H, ArH($_{19}$)), 8.18 (d, J =4.8 Hz, ^{2}H, ArH($_{23}$)), 8.35 (d, J=4.8 Hz, ^{2}H, ArH($_{18}$)), 9.672 (s, ^{3}H, OH($_{7,12,13}$)); ^{13}C NMR (400 MHz CDCl$_3$): δ 94.2 (C$_8$), 99.15 (C$_6$), 103.95 (C$_4$), 116.22 (C$_{11}$), 116.23 (C$_{14}$), 119.65 (C$_{10}$), 121.99 (C$_{15}$), 125.72 (C$_{17}$), 126.41 (C$_{22}$), 129.12 (C$_{24}$), 129.24 (C$_{19}$), 130.685 (C$_{23}$), 130.72 (C$_{18}$), 133.54 (C$_{25}$), 133.76 (C$_{20}$), 140.54 (C$_2$), 144.81 (C$_{12}$), 145.79 (C$_{13}$), 148.47 (C$_5$),153.34 (C$_1$), 153.46 (C$_9$), 161.1 (C$_7$), 166.21 (C$_{16}$), 166.32 (C$_{23}$), 176.13 (C$_3$); LC-MS, m/z: exact mass calculated for C$_{29}$H$_{16}$C$_{12}$O$_9$ is 578.02; found 578.92.

Synthesis of 2-(3,4-dihydroxyphenyl)-5,7-dihydroxy-4-oxo-4H-chromen-3-yl 4-methyl benzoate (QB4): Quercetin dihydrate (3 mmol), 4-methylbenzoic acid (8 mmol), zinc chloride (3 mmol) and 10 ml of phosphorous oxychloride was gradually added to

the RBF. The reaction mixture was stirred for 15 hrs at 75 °C. The reaction completion was supervised by TLC. Upon formation of the product, stopped stirring and the product was allowed to cool. Ice cold water was added and to extract the product ethyl acetate was used. The separated ethyl acetate layer was collected and evaporated. The obtained orange-yellow product was subjected to column chromatography using dichloromethane: ethyl acetate (50:50) as a mobile phase. The pure product was separated, collected and dried [10]. Yield: 127 mg (10.2%); m.p. 210-214 °C; FT-IR (cm^{-1}): 3295.21 (alcohol O-H stretch), 2924.18 (Ar-H), 2860.53 (aliphatic C–H stretch), 1743.71 (C=O stretch), 1680.05 (C=C stretch), 1143.53 (C-O ester); ^{1}H NMR (400 MHz CDCl$_3$): δ 2.61 (s, ^{3}H, ArH$_{(21)}$) 6.34 (s, ^{1}H, ArH$_{(6)}$), 6.62 (s, ^{1}H, ArH$_{(8)}$), 7.694 (s, ^{1}H, ArH$_{(11)}$), 7.82 (d, J=2 Hz, ^{1}H, ArH$_{(14)}$), 8.19 (d, J=1.2 Hz, ^{1}H, ArH$_{(15)}$), 8.40 (d, J=3.6 Hz, ^{2}H, ArH$_{(19)}$), 8.73 (d, J=2.4 Hz, ^{2}H, ArH$_{(18)}$), 10.16 (s, ^{3}H, OH$_{(7,12,13)}$), 12.18 (s, ^{1}H, OH(5)); ^{13}C NMR (400 MHz CDCl$_3$): δ 22.32 (C$_{21}$), 91.48 (C$_8$), 97.16 (C$_6$), 103.76 (C$_4$), 114.24 (C$_{11}$), 117.39 (C$_{14}$), 120.51 (C$_{15}$), 122.25 (C$_{10}$), 124.62 (C$_{17}$), 129.79 (C$_{19}$), 131.31 (C$_{18}$), 133.42 (C$_2$), 142.97 (C$_{20}$), 143.84 (C$_{12}$), 143.85 (C$_{13}$), 149.17 (C$_1$), 152.86 (C$_9$), 160.93 (C$_5$), 164.22 (C$_{16}$), 165.49 (C$_7$), 174.34 (C$_3$); LC-MS, m/z: exact mass calculated for C$_{23}$H$_{16}$O$_8$ is 420.08; found 420.06.

Physicochemical, pharmacokinetic and drug-likeness properties screening and prediction

The molecular descriptors, physicochemical properties and pharmacokinetic properties were evaluated using Swiss ADME web server (http://www.swissadme.ch/ accessed on 22 July 2021) [11], and Pre-ADME (https://preadmet.bmdrc.kr/) were used to predict physicochemical, lipophilicity, water solubility, pharmacokinetic and drug-likeness properties including Absorption, Distribution, Metabolism And Excretion (ADME) and toxicity. The screening criteria of drug-likeness compounds state that the synthesized compounds should be aqueous-soluble, should have high gastrointestinal absorption, orally active drug should satisfy Lipinski's rule of five and low human Ether-a-go-go-Related Gene (hERG) inhibition risk (low toxicity) [11].

Biological activity

In vitro antioxidant activity: The methods for *in vitro* antioxidant activity are based on the inhibition of free radicals. The inhibition of free radicals is measured when the samples are added to a system where free radicals are generated. The inhibition is relative to the antioxidant capacity of each sample. *In vitro* antioxidant methods provide an indication of antioxidant capacity of the compounds. In the present study, the synthesized quercetin derivatives were tested for *in vitro* antioxidant activity using DPPH and H$_2$O$_2$ assay.

Scavenging of H$_2$O$_2$ assay: A solution of H$_2$O$_2$ was prepared in phosphate buffer saline pH 7.4. Various concentrations (100-12.5 μg/ml) of samples and standards (ascorbic acid and quercetin) in methanol were prepared and added to H$_2$O$_2$ solution in PBS. After 10 min, the absorbance was measured at 230 nm [12,13].

Scavenging of DPPH assay: The 100 μM of DPPH solution was prepared using methanol. The different concentrations of standard (ascorbic acid and quercetin) and quercetin derivatives in Distilled Dimethyl Sulphoxide (DMSO) were prepared (100-12.5 μg/ml) and then added to DPPH solution. After 30 min, the absorbance for each was measured at 490 nm [12,13].

In vitro cytotoxicity by MTT assay method: *In vitro* cytotoxicity was carried out in the Animal Tissue Culture Laboratory, Department of Pharmaceutical Biotechnology at JSS College of Pharmacy, Ootacamund, Tamilnadu, India. The *in vitro* cytotoxicity study involved the determination of mitochondrial synthesis by MTT assay and was performed on MCF-7 breast cancer cell line.

Preparation of test solutions: All the quercetin derivatives (QB1-4) were dissolved in Distilled Dimethyl Sulphoxide (DMSO) separately and Dulbecco's Modified Eagle Medium (DMEM) was used to make volume with 2% inactivated Fetal Bovine Serum (FBS) to obtain a stock solution of 1000 μg/ml concentration and sterilized by filtration and stored at -20°C till use. Serial dilutions were made to obtain lower dilutions.

Cell lines and culture medium: MCF-7 cell line was procured from National Centre for Cell Sciences (NCCS), Pune, India. For culturing cell lines, DMEM supplemented with 10% inactivated FBS, Penicillin (100 IU/ml), Amphotericin B (5 μg/ml) and Streptomycin (100 μg/ml) were used in 5% CO$_2$ at 37°C in a humidified atmosphere. The cells were dissociated with Trypsin Phosphate Versene Glucose (TPVG) solution (0.2% trypsin, 0.02% Ethylene diamine tetraacetic acid, 0.05% glucose in phosphate buffer solution). The cultures were grown in 25 ml flat bottles and experiment was carried out in 96 well microtiter plates, considered as stock culture.

The monolayer cell culture was trypsinized and by using DMEM containing 10% FBS the cell count was adjusted to 1.0×10^5 cells/ml. The 0.1 ml of diluted cell line (approximately 10,000 cells) was added to a 96 well microtiter plate. The partial monolayer was formed after 24 hrs and the supernatant was flicked off. The monolayer was washed with DMEM medium. To the partial monolayer, 100 μl of different concentrations of synthesized compounds were added in microtiter plates. The plates were kept for incubation at 37°C for 72 hrs in 5% CO$_2$ atmosphere. The microscopic examination was carried out and in an every 24 hrs interval observations were made. The drug solutions in the wells were discarded after 72 hrs. 3-(4,5-Dimethylthiazol-2-yl)-2,5-diphenyltetrazolium bromide (MTT) in PBS (50 μl) was added to each well and gently shaken. The plates were again incubated for 3 hrs at 37°C in 5% CO$_2$ atmosphere. The supernatant was removed and 100 μl of propanol was added to the plates and gently shaken to solubilize the formed formazan. The plates were subjected for absorbance using a microplate reader at a wavelength of 540 nm. The percentage growth inhibition was calculated using the following formula and concentration of test drug needed to inhibit cell growth by 50% (CTC$_{50}$) values was generated from the dose-response curve of the selected cell line [14,15].

$$\%Growth\ inhibition = 100 - \left[\frac{Mean\ OD\ of\ individual\ test\ group}{(Mean\ OD\ of\ control\ group)} \times 100 \right]$$

Molecular docking: The X-ray crystallographic structure of human iNOS protein with resolution of 2.25 Å was collected from RCSB Protein Data Bank (PDB ID: 4NOS) and selected as the target protein for docking of the four designed compounds and quercetin. All the ligands were sketched using ChemDraw Professional 15.0 software. Ligand and protein were prepared and docking was done through BIOVIA Discovery Studio 2019 software. Molecular docking was performed using CDOCKER algorithm which is a simulated annealing docking method that uses CHARMm force field based molecular dynamics to generate random conformations. Different conformations for ligand adopting rigid body rotations were generated and CDOCKER energy and interaction energies (kcal/mol) for the molecules were obtained [16].

RESULTS AND DISCUSSION

Chemistry

After a thorough literature search and several trials and errors, we finally designed and carried out one-pot synthesis ester analogues of quercetin using benzoic acid and its derivatives namely o-chlorobenzoic acid, p-chlorobenzoic acid and p-methylbenzoic acid in the presence of phosphorusoxychloride and zinc chloride (Supplementary Figure 1). Compounds were obtained after purification by column chromatography and preparative Thin Layer Chromatography (TLC). The reaction of quercetin with benzoic acid in the presence of phosphorous oxychloride and zinc chloride catalyst afforded the quercetin-3-O-benzoic acid ester derivative (QB1). Purification was done by preparative TLC. The QB1 compound was obtained as a yellow solid (Table 1). The proton Nuclear Magnetic Resonance ^{1}H (NMR) spectra of QB1 showed 10 proton peaks. Characteristic singlet signals at δ 6.18, 6.45, and 7.47 ppm, doublet peaks at δ 7.74 and 8.13 ppm and triplet signals δ 7.59 and 7.93 ppm were observed and all corresponded to the aromatic protons, respectively. The two singlet signals at δ 9.32 and 12.46 ppm were assigned to the hydroxyl protons.

Treatment of quercetin dihydrate with o-chlorobenzoic acid in phosphorous oxychloride and catalyzed by zinc chloride yielded quercetin-3,5-O-2-chlorobenzoic acid ester derivative (QB2). The compound was purified by preparative TLC. The QB2 compound was obtained as a yellow solid. The ^{1}H NMR spectra of QB2 showed nine proton peaks. It displayed characterized singlet peaks at δ 6.03, 6.17 and 6.46 ppm, doublet signals at δ 6.73, 7.20, 8.08 and 8.23 ppm, and triplet peaks at δ 7.69 ppm were assigned for aromatic protons respectively. The singlet signal at δ 9.37 was assigned to the hydroxyl protons.

The reaction between quercetin dihydrate and p-chlorobenzoic acid in the presence of phosphorous oxychloride and zinc chloride yielded the formation of multiple products. The compound was separated and purified by column chromatography using suitable solvents. Quercetin-3,5-O-4-chlorobenzoic acid ester derivative (QB3) was a pale yellow color solid (Table 1). The ^{1}H NMR spectra of QB3 showed ten proton peaks. Spectra revealed singlet signals at δ 6.07, 6.25 and 6.54 ppm and doublet signals at δ 6.85, 7.25, 7.51, 7.74, 8.18 and 8.35 ppm were assigned to aromatic protons respectively. The singlet peak at δ 9.67 ppm was assigned to the hydroxyl protons. As per Supplementary Figure 1, quercetin dihydrate was treated with p-methylbenzoic acid in the presence of phosphorous oxychloride catalyzed by zinc chloride to form multiple products that were separated and purified by column chromatography to afford compound quercetin-3-O-4-methylbenzoic acid ester derivative (QB4) as a pale-yellow solid. The ^{1}H NMR spectra of QB4 integrated for ten proton peaks. Spectra displayed a characteristic singlet signal at δ 2.61 ppm assigned to CH$_3$ protons. The signals for aromatic protons appeared at δ 6.34, 6.62 and 7.69 ppm as singlet and 7.82, 8.19, 8.40 and 8.73 ppm as doublet. The singlet signals at δ 10.16 and 12.18 were assigned to the hydroxyl protons.

Physicochemical and drug-likeness properties

An attempt was made to determine the chance for synthesized quercetin derivatives to become an oral drug with the bioavailability of the molecule by analyzing physicochemical properties, water solubility, lipophilicity, pharmacokinetic and drug-likeness properties. These physicochemical parameters are for predicting the aqueous solubility, intestinal permeability and oral bioavailability of synthesized compounds.

In pharmacokinetic property screening and prediction, the synthesized derivatives should satisfy the binding affinity and ADMET screening selection criteria with eligible water solubility, high GI absorption, eligible drug-likeness and low the human Ether-a-go-go Related Gene (hERG) inhibition risk [17]. All the other chemical compounds were excluded due to unsuitable water solubility, GI absorption, drug-likeness and toxicity. The predicted results are summarized in Table 2.

The quercetin derivatives QB2 and QB3 were excluded due to high hERG inhibition risk, low GI absorption and violations of Lipinski's rules. The molecule QB and QB1 were included due to high GI absorption, no violations of Lipinski's rules and medium hERG inhibition risk whereas as QB4 was included for the reasons of GI absorption, one violation of Lipinski's rules i.e., Egan violations, and medium hERG inhibition risk. The detailed information such as pharmacokinetic property screening and prediction of synthesized quercetin derivatives are summarized in Table 2.

Biological activities

In vitro antioxidant activity: *In vitro* the antioxidant activity of synthesized compounds was performed on H$_2$O$_2$ and DPPH free radicals. Ascorbic acid was used as a standard. The half maximal Inhibitory Concentration (IC$_{50}$) values in H$_2$O$_2$ and DPPH assays for the tested compounds were shown in Table 3. The IC$_{50}$ values of the compounds suggested that the compounds QB1 and QB2 have shown potent activity for both H$_2$O$_2$ and DPPH scavenging and better activity than the standards used.

In vitro cytotoxicity studies: The synthesized compounds were evaluated for *in vitro* cytotoxicity against MCF-7 breast cancer cell lines using an 3-(4,5-Dimethylthiazol-2-yl)-2,5-diphenyltetrazolium bromide (MTT) assay. The percentage of cell viability was calculated and the concentration of test samples of synthesized compounds needed to inhibit cell growth by 50% values were calculated from the dose-response curves. The CTC$_{50}$ values for the tested compounds have been shown in Table 4. The Common Toxicity Criteria 50 (CTC$_{50}$) values showed that among all the synthesized compounds, QB2 showed remarkable cytotoxicity on breast cancer cells of MCF-7 when compared to 5-FU. In general, all four compounds have shown potent activity against MCF-7 cells.

Molecular docking studies: The four designed ligands and quercetin were docked with 4 NOS protein. Docking was performed using the CDOCKER algorithm in which docking estimation is done by calculating the - CDOCKER energy (based on receptor-ligand interaction energy and internal ligand strain energy) and -CDOCKER interaction energy (non-bonding interaction energy existing between the protein and ligand). The greater value of -CDOCKER energy and -CDOCKER interaction energy is a more favorable binding interaction between the ligand and the protein (Figures 2 and 3) and (Table 5).

Table 1: List of synthesized compounds and their physical characterization data

Cpd. Code	Structure	IUPAC Name	Mol. formula	Mol. weight	Yield	M. P (°C)	pKa	Drug-likeness model score
QB-1		2-(3,4-dihydroxyphenyl)-5,7-dihydroxy-4-oxo-4H-chromen-3-yl benzoate	$C_{22}H_{14}O_8$	406.35	80 mg (10%)	220	6.7	1.2
QB-2		2-(3,4-dihydroxyphenyl)-7-hydroxy-4-oxo-4H-chromen-3,5-diyl bis (2-chlorobenzoate)	$C_{29}H_{16}Cl_2O_9$	579.34	100 mg (8.7%)	230	5.56	1.2
QB-3		2-(3,4-dihydroxyphenyl)-7-hydroxy-4-oxo-4H-chromene-3,5-diyl bis(4-chlorobenzoate)	$C_{29}H_{16}Cl_2O_9$	579.34	154 mg (9%)	240	5.56	1.09
QB-4		2-(3,4-dihydroxyphenyl)-5,7-dihydroxy-4-oxo-4H-chromen-3-yl 4-methylbenzoate	$C_{23}H_{16}O_8$	420.37	127 mg (10%)	210	6.7	0.76
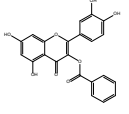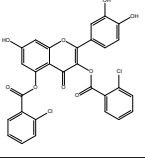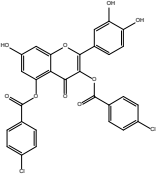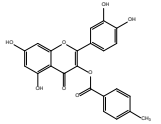
Table 2: Tahe screening and prediction of physicochemical properties, ADME, and toxicity of novel quercetin derivatives from PreADME and SwissADME.

Compound code	Physicochemical properties	Lipophilicity	Water solubility	Pharmacokinetics	Dru-likeness property	Toxicity	Eligibility
QB	MW: 302.24	iLOGP: 1.63	Log S(ESOL): -3.16	GI absorption: High	Lipinski violations: 0	Algae_at: 0.0378136	Yes
	Rotatable bonds: 1	XLOGP3: 1.54	Solubility (mg/ml) (ESOL): 2.11E-01	BBB permeant: No	Ghose violations: 0	Ames_test: Mutagen	
	H-bond acceptors: 7	WLOGP: 1.99	Solubility (mol/l) (ESOL): 6.98E-04	Pgp substrate: No	Veber violations: 0	Carcino_mouse: Negative	
	H-bond donors: 5	MLOGP: -0.56	Class (ESOL): Soluble	CYP1A2 inhibitor: Yes	Egan violations: 0	Carcino_rat: Positive	
	Molar refractivity: 78.03	Silicos-IT Log P: 1.54	Log S (Ali): -3.91	CYP2C19 inhibitor: No	Muegge violations: 0	daphnia_at: 0.214345	
	TPSA: 131.36	Consensus Log P: 1.23	Solubility (mg/ml) (Ali): 3.74E-02	CYP2C9 inhibitor: No	Bioavailability Score: 0.55	hERG_inhibition: Medium_risk	
			Solubility (mol/l)(Ali): 1.24E-04	CYP2D6 inhibitor: Yes		Medaka_at: 0.0778806	
			Class (Ali): Soluble	CYP3A4 inhibitor: Yes		Minnow_at: 0.0335026	
			ESOL Log S: 2.178	log Kp (cm/s): -7.05		TA100_10RLI: Negative	
			ESOL solubility (mg/ml): 3.76E+00			TA100_NA: Positive	
			ESOL solubility (mol/l): 5.34E+00			TA1535_10RLI: Negative	
			ESOL Class: Soluble			TA1535_NA: Negative	

QB1	MW: 406.34	iLOGP: 2.16	ESOL Log S: -5.25	GI absorption: Medium	Lipinski violations: 0	Algae_at: 0.0131925	No
	Rotatable bonds: 4	XLOGP3: 4.15	ESOL solubility (mg/ml):2.27E-03	BBB permeant: No	Ghose violations: 0	Ames_test: Non-mutagen	
	H-bond acceptors: 8	WLOGP: 3.5	ESOL solubility (mol/l): 5.59E-06	Pgp substrate: No	Veber violations: 0	Carcino_mouse: Negative	
	H-bond donors: 4	MLOGP: 0.81	ESOL class: Moderately soluble	CYP1A2 inhibitor: Yes	Egan violations:1	Carcino_rat: Positive	
	Molar refractivity: 107.41	Silicos-IT log P: 3.04	Ali Log S: -6.74	CYP2C19 inhibitor: No	Muegge violations: 0	Daphnia_at: 0.0292081	
	TPSA: 137.43	Consensus log P: 2.73	Ali solubility (mg/ml): 7.33E-05	CYP2C9 inhibitor: Yes	Bioavailability score: 0.55	hERG_inhibition: High_risk	
			Ali solubility (mol/l): 1.80E-07	CYP2D6 inhibitor: No		Medaka_at: 0.00199657	
			Ali class: Poorly soluble	CYP3A4 inhibitor: No		Minnow_at: 0.00201817	
			ESOL Log S: -5.95	log Kp (cm/s):-5.83		TA100_10RLI: Negative	
			ESOL solubility (mg/ml): 4.55E-04			TA100_NA: Negative	
			ESOL Solubility (mol/l): 1.12E-06			TA1535_10RLI: Negative	
			ESOL class: Moderately soluble			TA1535_NA: Negative	
QB2	MW: 579.34	iLOGP: 3.45	ESOL Log S: -7.52	GI absorption: Low	Lipinski violations: 1	Algae_at: 0.000407838	No
	Rotatable bonds: 7	XLOGP3:6.4	ESOL solubility (mg/ml): 1.75E-05	BBB permeant: No	Ghose violations: 3	Ames_test: Non-mutagen	
	H-bond acceptors: 9	WLOGP:6.32	ESOL solubility (mol/l): 3.02E-08	Pgp substrate: No	Veber violations: 1	Carcino_mouse: Negative	
	H-bond donors: 3	MLOGP:3.2	ESOL class: Poorly soluble	CYP1A2 inhibitor: No	Egan violations: 2	Carcino_rat: Negative	
	Molar refractivity: 146.81	Silicos-IT log P:5.86	Ali Log S: -9.21	CYP2C19 inhibitor: Yes	Muegge violations: 1	Daphnia_at: 0.000810637	
	TPSA: 143.5	Consensus log P:5.05	Ali solubility (mg/ml): 3.61E-07	CYP2C9 inhibitor: No	Bioavailability score: 0.55	hERG_inhibition: High_risk	
			Ali solubility (mol/l): 6.22E-10	CYP2D6 inhibitor: No		Medaka_at: 2.83e-06	
			Ali class: Poorly soluble	CYP3A4 inhibitor: No		Minnow_at: 9.98E-06	
			ESOL Log S: 5.013339	log Kp (cm/s):-5.29		TA100_10RLI: Negative	
			ESOL solubility (mg/ml): 8.77E+00			TA100_NA: Negative	
			ESOL solubility (mol/l): 1.25E+01			TA1535_10RLI: Negative	
			ESOL class: Poorly soluble			TA1535_NA: Negative	

	MW: 579.34	iLOGP: 3.47	ESOL Log S: -7.52	GI absorption: Low	GI absorption: Low	Algae_at: 0.000343968	
	Rotatable bonds: 7	XLOGP3: 6.4	ESOL solubility(mg/ml): 1.75E-05	BBB permeant:No	BBB permeant:No	Ames_test: Non-mutagen	
	H-bond acceptors: 9	WLOGP: 6.32	ESOL solubility (mol/l): 3.02E-08	Pgp substrate: No	Pgp substrate: No	Carcino_mouse: Negative	
	H-bond donors: 3	MLOGP: 3.2	ESOL class: Poorly soluble	CYP1A2 inhibitor: No	CYP1A2 inhibitor: No	Carcino_rat: Negative	
	Molar Refractivity: 146.81	Silicos-IT log P: 5.86	Ali Log S: -9.21	CYP2C19 inhibitor:Yes	CYP2C19 inhibitor:Yes	Daphnia_at: 0.00078625	
QB3	TPSA: 143.5	Consensus log P: 5.05	Ali solubility (mg/ml): 3.61E-07	CYP2C9 inhibitor: No	CYP2C9 inhibitor: No	hERG_inhibition: Medium_risk	No
			Ali solubility (mol/l): 6.22E-10	CYP2D6 inhibitor: No	CYP2D6 inhibitor: No	Medaka_at: 2.66E-06	
			Ali class: Poorly soluble	CYP3A4 inhibitor: No	CYP3A4 inhibitor: No	Minnow_at: 8.02e-06	
			ESOL Log S: 5.013339	log Kp (cm/s):-5.29	log Kp (cm/s):-5.29	TA100_10RLI: Negative	
			ESOL solubility (mg/ml): 8.77E+00			TA100_NA: Negative	
			ESOL solubility (mol/l): 1.25E+01			TA1535_10RLI: Negative	
			ESOL class: Poorly soluble			TA1535_NA: Negative	
	MW: 420.37	iLOGP: 2.88	ESOL Log S: -5.55	GI absorption: Low	Lipinski violations: 0	Algae at: 0.00700385	
	Rotatable bonds:4	XLOGP3:4.51	ESOL solubility (mg/ml): 1.19E-03	BBB permeant: No	Ghose violations: 0	Ames_test: Non-Mutagen	
	H-bond acceptors:8	WLOGP:3.81	ESOL solubility (mol/l): 2.83E-06	Pgp substrate: No	Veber violations: 0	Carcino_mouse: Negative	
	H-bond donors:4	MLOGP:1.3	ESOL class: Moderately soluble	CYP1A2 inhibitor: Yes	Egan violations: 1	Carcino_rat: Positive	
	Molar Refractivity:112.38	Silicos-IT Log P: 3.57	Ali Log S: -7.12	CYP2C19 inhibitor: No	Muegge violations: 0	daphnia_at: 0.0182565	
QB4	TPSA:137.43	Consensus Log P:3.21	Ali solubility (mg/ml): 3.21E-05	CYP2C9 inhibitor: Yes	Bioavailability Score: 0.55	hERG_inhibition: Medium_risk	Yes
			Ali solubility (mol/l): 7.63E-08	CYP2D6 inhibitor: No		Medaka_at: 0.000814033	
			Ali class: Poorly soluble	CYP3A4 inhibitor: No		Minnow_at: 0.000942542	
			ESOL Log S: 3.7004	log Kp (cm/s):-5.66		TA100_10RLI: Negative	
			ESOL solubility (mg/ml): 6.48E+00			TA100_NA: Negative	
			ESOL solubility (mol/l): 9.25E+00			TA1535_10RLI: Negative	
			ESOL class: Moderately soluble			TA1535_NA: Negative	

Table 3: *In vitro* antioxidant activity of quercetin and its derivatives.

Standard/Compound code	IC$_{50}$ (µg/ml)*	
	H$_2$O$_2$ assay	DPPH assay
Ascorbic acid	50.14 ± 1.31	57.25 ± 0.35
Quercetin	54.34 ± 1.45	58.75 ± 0.5
QB-1	19.34 ± 1.82	36.02 ± 1.20
QB-2	80.73 ± 1.24	40.71 ± 1.83
QB-3	235.7 ± 1.34	138.23 ± 3.21
QB-4	139.85 ± 1.56	458.56 ± 4.28

Note: *Average of three determinations.

Table 4: *In vitro* cytotoxicity of synthesized quercetin derivatives against MCF-7.

Standard/Compound code	IC$_{50}$ (µg/ml)*
QB-1	54.28 ± 0.35
QB-2	9.42 ± 0.35
QB-3	29.32 ± 0.35
QB-4	83.47 ± 0.35
Quercetin	11.17 ± 0.35
5-FU	12.5 ± 0.35

Note: *Average of three determinations.

All the ligands efficiently docked with the protein target and displayed well -CDOCKER interaction energies (12.97 to 64.69 kcal/mol) as shown in Table 3. As shown in Figures 2A and 3A, the catechol hydroxyl group at the 4' position of quercetin formed a hydrogen bond with ARG B:381 with bond length of 5.54 Å. Pi-alkyl interactions with ILE B-462, MET B:120 and VAL B-465 residues were seen in quercetin. The -CDOCKER interaction energy was 23.31 kcal/mol and the -CDOCKER energy was 20.56 kcal/mole for quercetin.

In the molecular docking interaction study, QB1 showed a -CDOCKER interaction energy value of 57.99 kcal/mol and a -CDOCKER energy value of 48.72 kcal/mol. Conventional hydrogen bond interaction with TYR A:491, PRO A:350 and TRP A:372, Pi-Pi stacked and Pi-Pi T-shaped interaction with PHE A:369 and TRP A:194 and Pi-alkyl interaction with PRO B:467 and MET B:120, as shown in Figures 2B and 3B. Among all the ligands, QB2 showed the highest value of -CDOCKER interaction energy value of 64.69 kcal/mol and -CDOCKER energy value of 37.03 kcal/mol. In Figures 2C and 3C, the conventional hydrogen bond formation with TYR A:491, Pi-Pi stacking interaction with TRP A:463, PHE A:369 and TRP A-194, Pi-alkyl interaction with ALA A:197, PRO A:350 and MET A:355, and van der Waals interaction

with PHE A:488, TYR A:489, LEU A:209, TRP A:372, TYR A:373, GLY A:202 was found and has shown better interaction energy when compared with other quercetin derivatives. QB3 displayed a -CDOCKER interaction energy value of 60.29 kcal/mol and –CDOCKER energy value of 48.28 kcal/mol. From Figures 2D and 3D, it has been seen that the carbonyl oxygen of ester moiety formed a conventional hydrogen bond with ILE A:201 residue. Pi-sulfur interaction was found with TRP A:372 and PHE A:369 residue, Pi-alkyl interaction with ARG A:199, LEU A:125, TYR A:491, PHE A:488, MET A:374, PRO A:467, ARG A:381, and ALA A:197 residues.

Further, the -CDOCKER interaction energy and -CDOCKER energy for QB4 displayed was 51.33 kcal/mol and 40.32 kcal/mol respectively. A conventional hydrogen bond is formed with TYR A:373 and TYR A:491, Pi-anion interaction with GLU A:377 and ARG A:199, Pi-alkyl interactions with VAL A:352 and TRP A:372, and van der Waal's interaction with ASP A:382, TRP A:346, GLN A:263, ALA A:351, TRP A:463, MET A:355 (Figures 2E and 3E). Lastly, the docking study of standard drug 5-FU was observed and found to be conventional hydrogen bond with ARG A:381, TRP A:463 and Pi-sulfur bond with MET A:120 (Figures 2F and 3F).

Figure 2: A) 2D interaction of quercetin with 4 NOS; B) 2D interaction of QB-1 with 4 NOS; C) 2D interaction of QB-2 with 4 NOS; D) 2D interaction of QB-3 with 4 NOS; E) 2D interaction of QB-4 with 4 NOS; F) 2D interaction of 5-FU with 4 NOS; Orange denotes Pi-cation bonds, the bright and light pink represent Pi-Pi stacking or Pi-Pi T-shaped and Pi-alkylbonds, respectively and light and bright green denote the van der Waals interaction and the conventional hydrogen bonds, respectively.

Figure 3: A) 3D interaction of quercetin with 4 NOS; B) 3D interaction of QB-1 with 4 NOS; C) 3D interaction of QB-2 with 4 NOS; D) 3D interaction of QB-3 with 4 NOS; E) 3D interaction of QB-4 with 4 NOS F) 3D interaction of 5-FU with 4 NOS.

Table 5: CDOCKER scores of quercetin and its derivatives.

Standard/Compound code	−CDOCKER energy	−CDOCKER interaction energy
QB-1	48.72	57.99
QB-2	37.03	64.69
QB-3	48.28	60.29
QB-4	40.32	51.33
Quercetin	20.56	23.31
5-FU	5.61	12.97

CONCLUSION

Novel quercetin analogs were synthesized from quercetin by one-pot synthesis, purified and characterized. Physicochemical and drug-likeness properties were concluded for the eligibility of oral drugs. In the *in vitro* antioxidant and cytotoxicity studies, IC_{50} values revealed that compound QB1 was a potent antioxidant in both H_2O_2 scavenging and DPPH assay methods and the results were greater than those of the standards used. Compound QB2 highest cytotoxicity against the MCF-7 cancer cell line and the best docked ligand with good interaction energy and favorable interaction with the target enzyme 4 NOS. We conclude from the results of biological activities and docking studies that the QB1 and QB2 compounds can be further analyzed and optimized as future potential drug candidates for cancer treatment.

ACKNOWLEDGMENTS

CONFLICT OF INTEREST

The author declared no conflict of interest.

REFERENCES

1. Sharma N. Free radicals, antioxidants and disease. Biol Med. 2014;6(3):1.

2. David AV, Arulmoli R, Parasuraman S. Overviews of biological importance of quercetin: A bioactive flavonoid. Pharmacogn Rev. 2016;10(20):84.

3. Panche AN, Diwan AD, Chandra SR. Flavonoids: An overview. J Nutr Sci. 2016;5:e47.

4. Chen X, Yin OQ, Zuo Z, Chow MS. Pharmacokinetics and modeling of quercetin and metabolites. Pharm Res. 2005;22(6):892-901.

5. Rossi M, Rickles LF, Halpin WA. The crystal and molecular structure of quercetin: A biologically active and naturally occurring flavonoid. Bioorg Chem. 1986;14(1):55-69.

6. Cárdenas M, Marder M, Blank VC, Roguin LP. Antitumor activity of some natural flavonoids and synthetic derivatives on various human and murine cancer cell lines. Bioorg Med Chem. 2006;14(9):2966-2971.

7. Danihelová M, Veverka M, Šturdík E, Jantová S. Antioxidant action and cytotoxicity on HeLa and NIH-3T3 cells of new quercetin derivatives. Interdiscip Toxicol. 2013;6(4):209-216.

8. Lu C, Huang F, Li Z, Ma J, Li H, Fang L. Synthesis and bioactivity of quercetin aspirinates. Bull Korean Chem Soc. 2014;35(2):518-520.

9. Zhong D, Liu M, Cao Y, Zhu Y, Bian S, Zhou J, et al. Discovery of metal ions chelator quercetin derivatives with potent anti-HCV activities. Molecules. 2015;20(4):6978-6999.

10. Gurunadham G, Raju RM, Venkateswarlu Y. Simple and efficient esterification reaction catalyzed by Zinc Chloride ($ZnCl_2$). Int J Sci Res Publ. 2015;5(1).

11. Khan MF, Nahar N, Rashid RB, Chowdhury A, Rashid MA. Computational investigations of physicochemical, pharmacokinetic, toxicological properties and molecular docking of betulinic acid, a constituent of *Corypha taliera* (Roxb.) with Phospholipase A_2 (PLA_2). BMC complement Altern Med. 2018;18(1):1-5.

12. Badami S, Prakash O, Dongre SH, Suresh B. *In vitro* antioxidant properties of Solanum pseudocapsicum leaf extracts. Indian J Pharmacol. 2005;37(4):251.

13. Jayaprakasha GK, Rao LJ, Sakariah KK. Antioxidant activities of flavidin in different *in vitro* model systems. Bioorg Med Chem. 2004;12(19):5141-5146.

14. Alley MC, Scudiero DA, Monks A, Hursey ML, Czerwinski MJ, Fine DL, et al. Feasibility of drug screening with panels of human tumor cell lines using a microculture tetrazolium assay. Cancer Res. 1988;48(3):589-601.

15. Hoang TK, Huynh TK, Nguyen TD. Synthesis, characterization, anti-inflammatory and anti-proliferative activity against MCF-7 cells of o-alkyl and o-acyl flavonoid derivatives. Bioorg Chem. 2015;63:45-52.

16. Singh SP, Konwar BK. Molecular docking studies of quercetin and its analogues against human inducible nitric oxide synthase. SpringerPlus. 2012;1(1):1-69.

17. Sun Y, Yang AW, Hung A, Lenon GB. Screening for a potential therapeutic agent from the herbal formula in the 4th edition of the Chinese national guidelines for the initial-stage management of covid-19 *via* molecular docking. Evid Based Complement Alternat Med. 2020;2020.